Macromolecular Chemistry and Physics
www.mcp-journal.de

The Effect of mPEGA/EHA Ratio and Copolymer Composition on the Solution Behavior of Amphiphilic, Comb-Shape Copolymers Synthesized via Cu(0)-Mediated SET-LRP for Potential Drug Delivery Applications

*Yasaman Pourdakheli Hamedani, Semanur Çakırefe, Agnes Fietz, José Hurst, Sven Schnichels, and Friederike Adams**

Comb-shape, block copolymers from hydrophilic poly(ethylenglycol) monomethyl ether acrylate (mPEGA, A) and hydrophobic 2-ethylhexyl acrylate (EHA, B) are synthesized by copper(0)-mediated single-electron transfer living radical polymerization (SET-LRP) via sequential addition of the two monomers, resulting in different compositions (AB, ABA, BAB, BA), molar masses, and mPEGA/EHA ratios. All polymers show narrow molar mass distributions and molecular weights of 7.7–25.50 kg mol^{-1}, demonstrating precise control over the polymerization and molecular weights through the utilization of SET-LRP. Kinetic experiments are conducted to investigate the polymerization behavior of mPEGA and EHA in *N,N*-dimethylformamide as a rather uncommon solvent for SET-LRP further underlining a living-type polymerization. Amphiphilic properties are investigated by critical micelle concentration (CMC) measurements and formation of micelles in water. A reverse relation between mPEGA/EHA ratio and CMC values reveals that an increased hydrophobicity leads to decreased CMC values. The self-assembly behavior of polymers in water confirms the formation of uniform and stable micelles in water with a size between 12 and 184 nm depending on the composition of the polymers. With increased hydrophilicity, micelle sizes increase as well. In vitro tests of the obtained polymers show excellent biocompatibility even at high concentrations further affirming their suitability for drug delivery applications.

1. Introduction

Amphiphilic block copolymers that spontaneously form self-assembled nanostructures sparked a lot of attention as drug transporters.[1] Different types of nanostructures such as micelles,[2] liposomes,[3] polymersomes,[4] or dendrimers[5] can be created using different building blocks and preparation methods.[6] There has been a lot of interest in utilization of polymeric micelles delivery systems made of biocompatible, amphiphilic block copolymers.[7] Polymeric micelles, with their distinctive core–shell structure, are the most widely used nanoplatforms for drug delivery.[8] During self-assembly of amphiphilic polymers to micelles, hydrophobic tails form the core, whereas the hydrophilic parts are exposed to the surrounding aqueous environment (shell). The critical micelle concentration (CMC), a significant parameter, refers to the minimum concentration of polymer necessary for micelle formation. Determining the CMC is crucial for understanding the behavior and properties of the amphiphilic molecules.[9] Micelles have

Y. Pourdakheli Hamedani, A. Fietz, J. Hurst, S. Schnichels, F. Adams
Institute for Ophthalmic Research
University of Tübingen
Elfriede-Aulhorn-Strasse 7, 72076 Tübingen, Germany
E-mail: friederike.adams@ipoc.uni-stuttgart.de

S. Çakırefe, F. Adams
Chair of Macromolecular Materials and Fiber Chemistry
Institute of Polymer Chemistry
University of Stuttgart
Pfaffenwaldring 55, 70569 Stuttgart, Germany

The ORCID identification number(s) for the author(s) of this article can be found under https://doi.org/10.1002/macp.202300226

DOI: 10.1002/macp.202300226

a soft and dynamic core-corona interaction because the integrated molecules are in equilibrium with free polymeric chains.[10] They are also often used due to their small size, simple preparation, sterilization methods, and effective dissolving.[11] It has been demonstrated that micelles between 30 and 100 nm in size can pass through highly permeability tumors; however, that only micelles with a dimension of 30 nm can pass through less permeability tumors.[12] Due to their core–shell structure, an advantage of micelles is their encapsulation and protection of hydrophobic drugs, targeted delivery, and controlled release.[10b] Amphiphilic block copolymers are constructs using a variety of hydrophilic and hydrophobic polymers.[8] The hydrophobic part can be made of polyesters like poly(ϵ-caprolactone) or poly(amino acids), such as poly(*L*-aspartate). Poly(ethylenglycol) (PEG) is typically used to serve as the hydrophilic component; however, other polymers can also be used, such as poly(vinyl pyrrolidone), poly(acryloylmorpholine), or poly(trimethylene carbonate).[12a] The surface properties of micelles, which control their stability, also have a significant effect on their behavior.[13] A neutral and hydrophilic surface lengthens circulation duration and regulates protein corona development. In addition, polymeric micelles can be designed to release drugs in a controlled manner, either through stimuli-responsive or sustained-release mechanisms, due to their hydrophobic core. This can optimize the pharmacokinetics and pharmacodynamics of drugs, leading to improved therapeutic outcomes.[11] Moreover, the hydrophobic core surrounding the micelles can improve the solubility and stability of hydrophobic drugs which can improve the bioavailability and efficacy of the drug.[14]

An efficient polymerization process for the controlled synthesis of well-defined polymers from a wide range of monomers is the copper(0)-mediated single-electron transfer living radical polymerization (SET-LRP). [15] A common type of catalyst is Cu(0)-wire, which can be a better option than Cu(0)-particles since it offers more effective molecular weight control, improved stability, and recyclability.[16] Furthermore, the copper-wire can easily be removed which results in lower levels of copper residues in the final products, allowing the material to be used directly in applications where copper contaminations are undesirable, such as drug delivery applications.[16] Due to its living-type polymerization characteristics it is also used for the synthesis of various types of functional polymers, including block copolymers. Acrylates and methyl acrylate are by far the most researched monomers.[17] Additionally, a wide range of solvents have been used under SET-LRP conditions, with dimethylsulfoxide (DMSO) and water being the most used solvents for hydrophilic and slightly hydrophobic monomers.[16]

Poly(ethylenglycol) monomethyl ether acrylate (mPEGA) and 2-ethylhexylacrylate (EHA) are readily available monomers and have not yet been combined in copolymers despite their promising properties for forming amphiphilic polymers. EHA is an important basic monomer for the synthesis of acrylate adhesives and hydrophobic coatings.[18] It serves as a versatile building block that copolymerizes with a wide variety of other acrylic monomers to tailor specific copolymer properties for a diverse range of nonrigid applications and should also be investigated in matters of drug delivery applications. The side chain of EHA with its ethyl branch and long length will generate additional hydrophobic–hydrophobic interactions. It will also prevent a compact order of the formed AB diblock copolymers. Reports have shown that using branched alkyl chains instead of linear ones in nonionic surfactants can have a major impact on interfacial properties as tail–tail interactions, steric effects, areas occupied by the surfactant at the interface, and tail hydrophobicity are varied. Branching can affect CMC values, aggregation behavior and micelle sizes.[19] It is also advantageous that 2-ethylhexyl acrylate can be prepared with a high yield by esterification of acrylic acid with 2-ethylhexanol thus being a cheap monomer which is also of major interest for chemical industry.[20] The lack of studies on efficient EHA SET-LRP and combination with hydrophilic monomers might be due to the insolubility of highly hydrophobic EHA in commonly used solvents DMSO and water.

Careful considerations for selecting an appropriate solvent, ligand, and initiator for the polymerizations is crucial for the success of the method.[21] In this study, anhydrous *N,N*-dimethylformamide (DMF) was chosen to replace the commonly used DMSO. After performing kinetic investigations to validate that both monomers, mPEGA and EHA, show excellent polymerization kinetics under the chosen conditions (Cu(0)-wire, DMF, $CuBr_2$, ME_6TREN, room temperature), block and random polymers with different architectures (AB, BA, ABA, and BAB), mPEGA/EHA ratios and molar masses were synthesized. The present work is focused on understanding the solution behavior of self-assembled nanostructures from these P(mPEGA-EHA) copolymers. Various complementary techniques, such as dynamic light scattering (DLS), CMC measurements, and transmission-electron microscopy (TEM) were employed to elucidate the formation of micelles from these amphiphilic polymers in dependence of their molar masses, arrangement of blocks/monomers and mPEGA/EHA ratios. Biocompatibility assessment was conducted using different methods such as 3-(4,5-dimethylthiazol-2-yl)−5-(3-carboxymethoxyphenyl)−2-(4-sulfophenyl)−2H-tetrazolium salt (MTS), crystal violet (CV), and calcein AM (AM = acetoxymethyl)/propidium iodide (PI) staining proving excellent biocompatibility profiles even at very high concentration (1000 μg mL^{-1}) after 24 and 48 h.

2. Result and Discussion

2.1. Polymerization Results

mPEGA and EHA were employed in Cu(0)-mediated SET-LRP to evaluate general activities, suitability of the chosen conditions for both monomers and microstructures of the isolated polymers. The polymerization reactions were carried out at room temperature in an argon-filled glove box. Cu(0)-wire was used as the catalyst, $CuBr_2$ as a deactivator, degassed Me_6TREN as ligand, degassed EbiB as the initiator and anhydrous, degassed DMF as solvent with a target degree of polymerization (DP) of 50 and a fixed ratio of 1:0.05:0.18 of EbiB:$CuBr_2$:Me_6TREN. Both monomers were only degassed and otherwise used as received (Figure S1 and S2, Supporting Information).

The reason for using DMF as a rather uncommon solvent in SET-LRP is that EHA was found to be immiscible with DMSO, whereas it exhibited good miscibility with DMF. Furthermore, trifluoroethanol, the only solvent that was yet used for SET-LRP of EHA, was excluded as an alternative because it is far more toxic

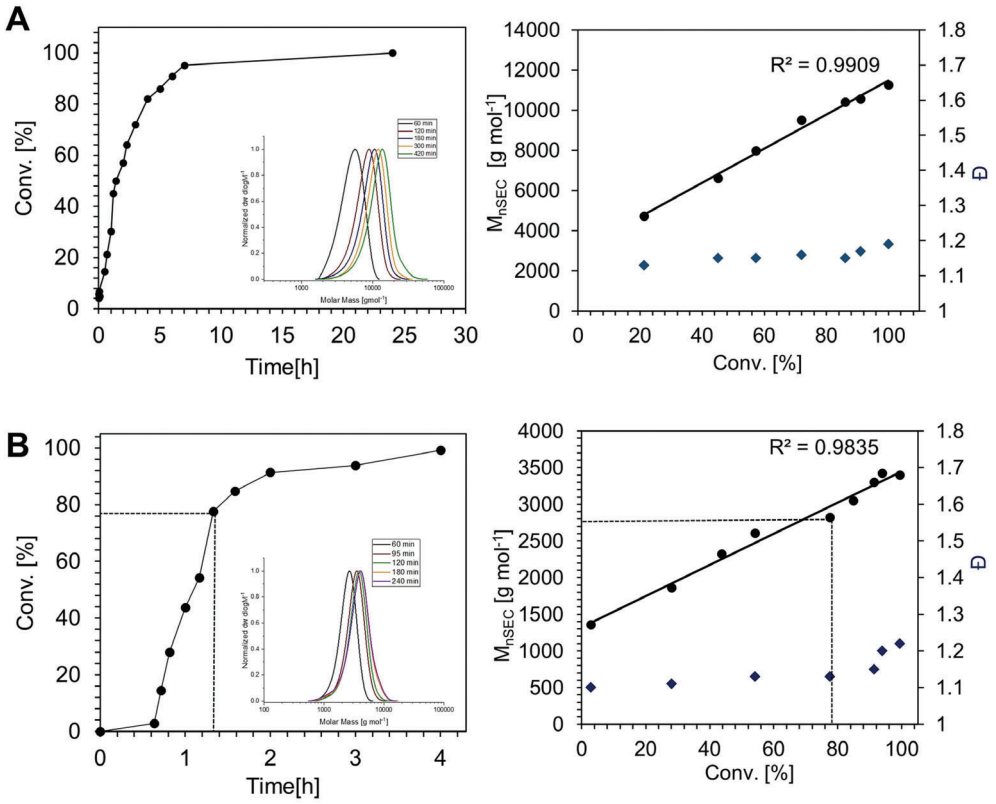

Figure 1. Polymerization kinetics by an aliquot method of A) mPEGA and B) EHA with a target DP of 50 and a fixed ratio of 1:0.05:0.18 of EBiB:$CuBr_2$:Me_6TREN with 5 cm Cu(0)-wire. Left: Conversion, determined by ^{1}H-NMR measurements, over reaction time for the polymerization besides growth of number-average molar mass, determined by SEC. Right: Dependency of M_n and $Đ$ on the conversion detmerined by SEC. Dotted lines in (B) show the timepoint from which on a two-phase system was observed.

than DMF and therefore unsuitable for potential drug delivery applications of the polymers.[15]

Kinetic experiments for each monomer were caried out to investigate the conversion of monomers, molar masses, and mass distributions of the obtained polymers (**Figure 1**). To determine conversions and kinetic parameters of the polymerization, aliquots were taken at regular time intervals during polymerization. The conversion was calculated using ^{1}H-NMR spectroscopy. Relative molar masses and mass distributions were measured by size-exclusion chromatography (SEC). The polymerization of mPEGA proceeded in a controlled manner, as indicated by narrow polydispersities ($1.13 \leq Đ \leq 1.19$) (Figure 1A). The plot of conversion against molecular weight revealed a linear relationship between M_n and conversion, further highlighting the living fashion of the polymerization. If the conversion is plotted against time, the polymerizations can be compared with regard to the activity of the SET-LRP system in mPEGA polymerization. Full conversion (≥ 99%) was reached after 7 h and a high conversion of 80% was already reached after 5 h. Since mPEGA with nine ethylenglycol-repeating unit in its sidechain, calculated from ^{1}H-NMR spectroscopy of the purchased monomer (Figure S1, Supporting Information), is a very sterically demanding monomer resulting in a comb-shape polymer, a lower activity of polymerization with a DP of 50 was expected. ^{1}H-NMR spectroscopy confirmed that the same number of repeating units per monomer unit is still present in the obtained P(mPEGA); thus no degradation of the side-chain occurred (Figure S3, Supporting Information).

After successful polymerization of mPEGA, the same polymerization setup was used for EHA homopolymerization to screen possible reaction conditions for block copolymerization of mPEGA with EHA. In similarity to mPEGA kinetic measurements, EHA was polymerized with the same aliquot method with the identical target DP of 50 resulting in a low molecular weight-polymer due to a lower molecular weight of the monomer (Figure 1B). It was noticed that the EHA chain started to grow after an induction period of around 40 min. In the context of earlier investigations, it was already observed that polymerizations with Cu(0)-wire can lead to an induction period time.[22] Full conversion (≥ 99%) was observed after 4 h and a high conversion of above 80% already after 1.5 h. In contrast to P(mPEGA), poly(2-ethylhexylacrylate) (P(EHA)) is not fully miscible with DMF. After 80 min, a two-phase system was observed leading to an increase in polydispersity of 1.21 and a slight inaccuracy in determining the monomer conversion and molar masses. However, since the Cu(0)-mediated SET-LRP is a surface polymerization on the copper wire, polymerization results were satisfactory. For both monomers, residual inhibitor that was not removed prior to polymerization did not seem to negatively influence polymer characteristics, making SET-LRP of commercially available monomers a convenient technique for effortless production of materials for drug delivery applications. Comparable results as

Table 1. Polymerization results of copolymerization of mPEGA with EHA resulting in AB, BA, and random copolymers.

Entry[a]		EBiB/mPEGA/EHA	Time$_1$[b] [h]	Conv.$_1$[c] [%]	M_{n1}[d] [x10^3 gmol^{-1}]	$Đ_1$[d]	Time$_2$[b] [h]	Conv.$_2$[c] [%]	M_{n2}[d] [x10^3 gmol^{-1}]	$Đ_2$[d]	Ratio of mPEGA/EHA[e]
1	P(mPEGA$_{10}$-*b*-EHA$_{47}$)	1/10/47	4	>99	3.0	1.18	19	>99	8.5	1.13	1:4.7
2	P(mPEGA$_{15}$-*b*-EHA$_{75}$)	1/15/75	4	98	4.8	1.11	26	>99	11.7	1.19	1:5.0
3	P(mPEGA$_{20}$-*b*-EHA$_{60}$)	1/20/60	4	98	5.8	1.13	26	>99	11.4	1.25	1:2.9
4	P(mPEGA$_{20}$-*st*-EHA$_{48}$)	1/20/48	–	–	–	–	20	>99	7.7	1.15	1:2.4
5	P(mPEGA$_{25}$-*b*-EHA$_{53}$)	1/25/53	4	99	6.2	1.11	26	>99	11.6	1.15	1:2.1
6	P(mPEGA$_{50}$-*b*-EHA$_{11}$)	1/50/11	4	99	9.9	1.10	26	>99	12.0	1.14	1.0.2
7	P(mPEGA$_{50}$-*b*-EHA$_{16}$)	1/50/16	4	87	8.4	1.12	19	>99	10.0	1.11	1:0.3
8	P(mPEGA$_{50}$-*b*-EHA$_{26}$)	1/50/26	4	97	9.2	1.13	26	>99	13.6	1.16	1:0.5
9	P(mPEGA$_{50}$-*b*-EHA$_{50}$)	1/50/50	4	>99	8.5	1.12	18	>99	12.112	1.15	1:1.0
10	P(EHA$_{50}$-*b*-mPEGA$_{50}$)	1/50/50	4	>99	3.8	1.19	19	>99	14.7	1.73	1:1.0
11	P(mPEGA$_{50}$-*b*-EHA$_{116}$)	1/50/116	4	96	8.6	1.10	16.5	>99	18.9	1.11	1:2.3
12	P(mPEGA$_{100}$-*b*-EHA$_{24}$)	1/100/24	24	98	17.1	1.13	20	71	19.5	1.13	1:0.3
13	P(mPEGA$_{100}$-*b*-EHA$_{111}$)	1/100/111	7	86	14.6	1.10	17	>99	25.5	1.08	1:1.1

[a] Ratio of 1:0.05:0.18 (EBiB:CuBr$_2$:Me$_6$TREN), room temperature, 2.25 mL DMF. Cleaned Cu(0)-wire (5 cm) was wrapped around the magnetic stir bar. EBiB/mPEGA/EHA = monomer feed ratio. P(mPEGA$_n$-*b*-EHA$_m$), P(mPEGA$_n$-*st*-EHA$_m$) P(EHA$_n$-*b*-mPEGA$_m$) with *n* and *m* based on the feed ratio and monomer conversions determined from the second aliquot. Polymers are arranged in order of increased mPEGA and EHA amount [b] Reaction time of the respective blocks [c] Calculated via ^{1}H-NMR spectroscopy (see the Supporting Information for more information). First monomer showed full conversion after chain extension [d] Relative molecular weight (M_n) and $Đ = M_w/M_n$ as determined via SEC in chloroform [e] Molar ratio of mPEGA/EHA according to ^{1}H-NMR-spectroscopy (700 MHz) (see the Supporting Information for more information).

for the kinetic measurements were obtained for P(mPEGA) and P(EHA) with a DP of 50 produced in a standard homopolymerization setup without taking aliquots validating the results from kinetic measurements (Table S1, Supporting Information).

Owing to the good control and living-nature of the SET-LRP technique, amphiphilic block copolymers with two (AB and BA, **Table 1**) and three blocks (ABA and BAB, **Table 2**) were produced by sequential addition of monomers after the previous one is nearly or entirely consumed (**Figure 2**). Aliquots of the first block were used to determine the conversion via ^{1}H- NMR measurements. Molar masses and polydispersities were determined from the same aliquot using SEC, likewise for a second or third aliquot of respective chain extensions. The same conditions as for the homopolymerizations were used because both monomers could successfully be polymerized with low polydispersities facilitating block copolymerizations. Various addition sequences, monomer ratios and target molar masses were chosen to obtain polymers with different copolymer composition, monomer ratios, and molar masses. The first block was always stirred for 4 h before addition of the second monomer. Only when a high amount of mPEGA was used as a first block (Table 1, Entries 12 and 13), polymerizations times were increased to 7–24 h. For all copolymerizations, the first monomer reached above 86% and, in most cases, full conversion before adding the second monomer. Regarding the chain extension in AB and BA polymerizations, monomer conversions were quantitative, except from P(mPEGA$_{100}$-*b*-EHA$_{24}$) in which EHA had a conversion of 71% conversion. Full conversion of the first monomer was always reached after copolymerization with the second monomer as determined from the second aliquot. Similar observations were made for ABA and BAB polymers, in which the monomer incorporated as second block was nearly (≥ 93%) and as the third block fully converted to polymer. All monomers showed full conversion in the third aliquot. Based on the monomer feed, the determined conversions and NMR-spectroscopy polymer compositions and ratios of mPEGA/EHA were determined (Tables 1 and 2 and Figure S5, Supporting Information). Figure 2C exemplifies an ^{1}H-NMR spectrum of a purified P(mPEGA-*b*-EHA). These NMR spectra were used for calculating the mPEGA/EHA ratio and also verified that all signals of the two single homopolymers are present in copolymers and no degradation of the PEG-repeating units took place. It was shown that the obtained ratios were in accordance with the monomer feed, thus, polymer compositions can easily be tailored by the monomer feed ratios as shown by synthesis of a wide variety of polymers with various mPEGA/EHA ratios. mPEGA/EHA ratios from 1:5 to 1:0.3 could precisely be targeted as well as molar masses between 7.7 and 25.5 kg mol^{-1}. Precise block copolymer formation was proven by SEC measurements and diffusion-ordered spectroscopy (DOSY) NMR studies. DOSY NMR spectra were recorded to prove the linkage of the different blocks on basis of the diffusion coefficient. These spectra showed only one set of signals and thus only one diffusion coefficient attributed to a formed block copolymer (Figure S6, Supporting Information). The successful synthesis of AB and ABA copolymers was also confirmed by absence of two distinct signals and a shift of the signal trace towards higher molar masses in SEC chromatograms (Figure 2A,B and Figure S7, Supporting Information). Solely, for the BA polymer P(EHA$_{50}$-*b*-mPEGA$_{50}$), a small signal attributed to P(EHA) homopolymer is still visible in the block copolymers, probably due to the formation of a two-phase system when EHA is polymerized as the first block leading to unreactive P(EHA). This copolymer was also the only sample with an increased polydispersity of 1.73. Consequently, only one BA and one BAB polymer were synthesized. For all other polymers, mPEGA was chosen as the first block due to a better polymerization control. These diblock polymers

Table 2. Polymerization results of copolymerization of mPEGA with EHA resulting in ABA and BAB polymers.

Entry[a]		EBiB/mPEGA/EHA	$Time_1$[b] [h]	$Conv._1$[c] [%]	M_{n1}[d] [x10^3 gmol^{-1}]	$Đ_1$[d]	$Time_2$[b] [h]	$Conv._2$[c] [%]	M_{n2}[d] [x10^3 gmol^{-1}]	$Đ_2$[d]	$Time_3$[b] [h]	$Conv._3$[c] [%]	M_{n3}[d] [x10^3 gmol^{-1}]	$Đ_3$[d]	Ratio of mPEGA/EHA[e]
1	P(mPEGA$_{25}$-*b*-EHA$_{55}$-*b*-mPEGA$_{25}$)	1/25/55/25	4	99	5.9	1.11	19	>99	9.78	1.09	23	>99	14.4	1.27	1:1.1
2	P(EHA$_{25}$-*b*-mPEGA$_{50}$-*b*-EHA$_{20}$)	1/25/50/20	4	99	1.8	1.20	15	92	16.2	1.14	24	>99	24.7	1.10	1:0.9

[a] Ratio of 1:0.05:0.18 (EBiB:$CuBr_2$:Me_6TREN), room temperature, 2.25 mL DMF. Cleaned Cu(0)-wire (5 cm) was wrapped around the magnetic stir bar. EBiB/mPEGA/EHA = monomer feed ratio. P(mPEGA$_n$-*b*-EHA$_m$-*b*-mPEGA$_n$) or P(EHA$_n$-*b*-mPEGA$_m$-*b*-EHA$_n$) with *n* and *m* based on the feed ratio and monomer conversions determined from the third aliquot [b] Reaction time of the respective blocks [c] Calculated via ^{1}H-NMR spectroscopy (see the Supporting Information for more information). All monomers showed full conversion after last chain extension [d] Relative molecular weight (M_n) and $Đ = M_w/M_n$ as determined via SEC in chloroform [e] Molar ratio of mPEGA/EHA according to ^{1}H-NMR-spectroscopy (700 MHz) (see the Supporting Information for more information).

had low polydispersities with slightly increased values when polymers contained higher amounts of EHA. For comparison reasons, one random copolymer was synthesized. P(mPEGA$_{20}$-*st*-EHA$_{48}$) showed a lower polydispersity than a similar AB block-copolymer (1.15 vs 1.30, Table 1, Entries 3 and 4) indicating that EHA had less influence on the control of the polymerization, probably because a formation of a hydrophobic block was inhibited.

2.2. Solution Behavior of Copolymers

The solubility behavior of polymers in chloroform was studied by using the DOSY NMR spectra (Figure S6, Supporting Information). In general, it is possible to estimate the molecular weight of a polymers from its diffusion coefficient obtained by DOSY-NMR spectroscopy, using the SEGWE (Stokes-Einstein Gierer-Wirtz estimation) method.[23] However, this calculation is most accurate for small molecules (<1000 g mol^{-1}) and the relationship between diffusion coefficients and molecular weights can be very complex. Nevertheless, we calculated the molecular weights and the hydrodynamic radii from diffusion coefficients using SEGWE (Table S2, Supporting Information). Molecular weights from DOSY NMR were too high in comparison to calculated ones due to the aforementioned restrictions in measuring high molecular weight species. Hydrodynamic radii indicate that there is barely any self-assembly in organic solvent chloroform. Solely triblock polymers, P(EHA$_{25}$-*b*-mPEGA$_{50}$-*b*-EHA$_{20}$) and P(mPEGA$_{25}$-*b*-EHA$_{55}$-*b*-mPEGA$_{25}$), showed radii around 5 nm which could indicate some formation of slightly bigger aggregates. Except from P(mPEGA$_{50}$-*b*-EHA$_{50}$), diffusion coefficients decrease and molecular weights and hydrodynamic radii increase with increasing calculated molecular weights. Similar trends were observed with the hydrodynamic diameter calculated from DLS in chloroform. Values were in general lower in these DLS measurements, further indicating that there is no micelle formation due to the solubility of both blocks in organic solvents such as chloroform.

The solubility of polymers in water was influenced by both the proportion of hydrophilic and hydrophobic components and the arrangement of monomers in the polymer chain. We also assume that the branched structure of EHA can have a positive impact on self-assembly characteristics. Hydrophobic chains with branched structure can provide a more complicated and complex micelle core structure. Due to the greater volume that may be available within the core as a result of the branching, higher drug loading in the core of the formed micelles could be facilitated. Within this context, it was observed that the AB and ABA block copolymer, characterized by an equivalent ratio of the two monomers (mPEGA/EHA ratio = 1:1 and 1:1.1, respectively), exhibited good solubility in water, whereas the BAB block copolymer with the same amount of hydrophilic and hydrophobic content (mPEGA/EHA ratio = 1:0.9), but different structure, was insoluble in water (**Table 3**, Entries 9, 14, 15). Interestingly, this behavior was not observed when comparing the AB and BA block copolymers with the same ratio of 1:1, as both polymers displayed water solubility (Table 3, Entries 9 and 10). This variation is probably attributed to a higher impact of the hydrophobic block when it is located on both ends of the polymer chain as observed in BAB

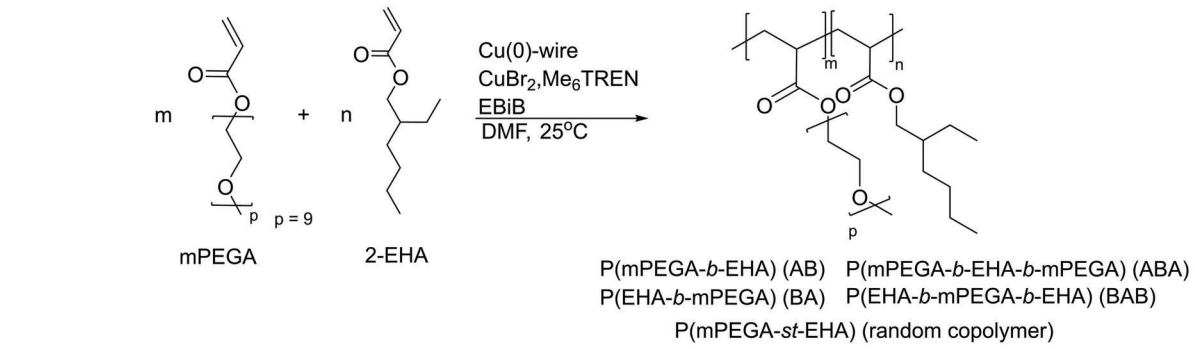

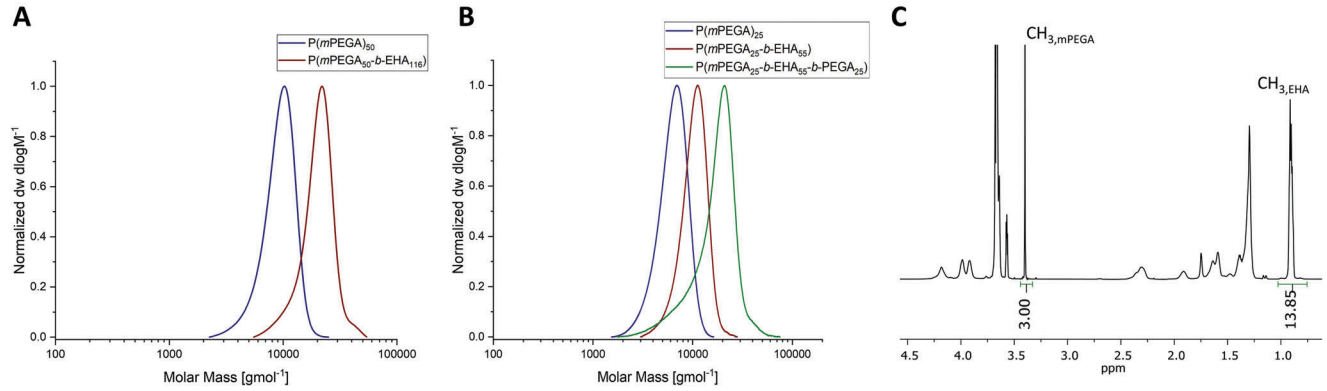

Figure 2. Top: Synthesis route of copolymers containing mPEGA and EHA by Cu(0)-mediated SET-LRP. Bottom: A) SEC analysis of P(mPEGA$_{50}$-*b*-EHA$_{116}$). B) SEC analysis of P(mPEGA$_{25}$-*b*-EHA$_{55}$-*b*-mPEGA$_{25}$). C) ^{1}H-NMR spectra of P(mPEGA$_{50}$-*b*-EHA$_{116}$) for calculation of mPEGA/EHA ratio by integration of the OCH$_3$-group of mPEGA and the two CH$_3$-groups of EHA.

Table 3. Solution behavior of copolymers as determined by hydrodynamic diameters ($Đ_h$), polydispersities (PDIs) and CMC values.

Entry		Hydrophilic/hydrophobic ratio[a)]	M_n[b)] [x10^3 g mol^{-1}]	$M_{n,calculated}$[c)] [x10^3 g mol^{-1}]	$Đ_h$ [nm] at 25 °C[d)]	PDI[d)]	CMC values[e)] [mg mL^{-1}]	CMC values[f)] [x10^{-7} M]
1	P(mPEGA$_{10}$-*b*-EHA$_{47}$)	1:4.7	8.5	13.5	–[g)]	–[g)]	–[g)]	–[g)]
2	P(mPEGA$_{15}$-*b*-EHA$_{75}$)	1:5	11.7	21.1	–[g)]	–[g)]	–[g)]	–[g)]
3	P(mPEGA$_{20}$-*b*-EHA$_{60}$)	1:3	11.4	20.7	–[g)]	–[g)]	–[g)]	–[g)]
4	P(mPEGA$_{20}$-*st*-EHA$_{48}$)	1:2.4	7.7	18.5	183.7 ± 4.43	0.20 ± 0.012	0.036	19
5	P(mPEGA$_{25}$-*b*-EHA$_{53}$)	1:2.1	11.6	21.5	36.44 ± 0.26	0.18 ± 0.009	0.041	19
6	P(mPEGA$_{50}$-*b*-EHA$_{11}$)	1:0.2	12.0	26.2	11.75 ± 0.55	0.26 ± 0.009	0.272	100
7	P(mPEGA$_{50}$-*b*-EHA$_{16}$)	1:0.3	10.0	27.1	14.45 ± 0.27	0.20 ± 0.027	0.186	68
8	P(mPEGA$_{50}$-*b*-EHA$_{26}$)	1:0.5	13.6	28.9	17.81 ± 3.63	0.16 ± 0.007	0.079	27
9	P(mPEGA$_{50}$-*b*-EHA$_{50}$)	1:1	12.1	33.3	34.81 ± 0.69	0.25 ± 0.003	0.045	13
10	P(EHA$_{50}$-*b*-mPEGA$_{50}$)	1:1	14.7	33.3	84.61 ± 0.57	0.25 ± 0.008	0.048	14
11	P(mPEGA$_{50}$-*b*-EHA$_{116}$)	1:2.3	18.9	45.5	53.24 ± 0.40	0.25 ± 0.117	0.057	12
12	P(mPEGA$_{100}$-*b*-EHA$_{24}$)	1:0.3	19.5	52.6	31.66 ± 0.43	0.24 ± 0.006	0.118	22
13	P(mPEGA$_{100}$-*b*-EHA$_{111}$)	1:1.1	25.5	68.7	54.64 ± 0.40	0.17 ± 0.007	0.138	20
14	P(mPEGA$_{25}$-*b*-EHA$_{55}$-*b*-mPEGA$_{25}$)	1:1.1	14.4	33.3	38.37 ± 0.33	0.26 ± 0.006	0.029	8
15	P(EHA$_{25}$-*b*-mPEGA$_{50}$-*b*-EHA$_{20}$)	1:0.9	24.7	33.3	–[g)]	–[g)]	–[g)]	–[g)]

[a)] Hydrophilic/hydrophobic ratio as observed from molar ratio of mPEGA/EHA according to ^{1}H-NMR-spectroscopy (700 MHz) [b)] Relative molecular weight (M_n) as determined via SEC in chloroform relative to polystyrene [c)] $M_{n,calculated}$ according to the monomer feed and mPEGA/EHA using the molecular weights of each monomer. Differences between M_n and $M_{n,calculated}$ are due to the calibration of the SEC setup with polystyrene standards [d)] Determined by dynamic light scattering (DLS) with polymer solution concentrations of 1.0 mg mL^{-1} at 25 °C [e)] CMC values obtained by Nile red method (see the Supporting Information for further information) [f)] CMC values calculated in [*M*] based on $M_{n,calculated}$ [g)] Polymers are insoluble in water.

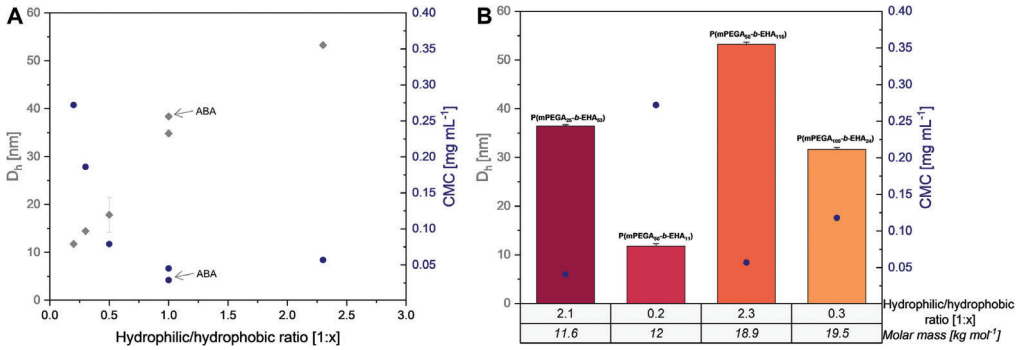

Figure 3. A) Hydrodynamic diameter (D_h) and CMC values obtained for P(mPEGA-*b*-EHA) copolymers with a fixed amount of the hydrophilic mPEGA block (DP = 50) and various amounts of hydrophobic EHA content as determined by the hydrophilic-to-hydrophobic ratio [1:*x*] with *x* being the EHA proportion in the polymers plotted on the *x*-axis. B) Hydrodynamic diameter (D_h) and CMC values obtained for P(mPEGA-*b*-EHA) copolymers with different mPEGA/EHA ratios and molar masses. Molar masses and the EHA fraction in the hydrophilic-to-hydrophobic ratio plotted on the *x*-axis.

polymers. Moreover, all other AB polymers with a higher proportion of hydrophilic components (mPEGA/EHA ratio 1:*x* with $x \leq 2.4$, x = proportion of EHA) demonstrated solubility in water. Thus, diblock copolymers with up to 70 mol% hydrophobic content were still soluble in water.

DLS was utilized to determine the hydrodynamic diameter ($Đ_h$) and PDI of the micelles by simply dissolving the polymers in water. A range of average hydrodynamic diameters from 12 to 184 nm was observed at 25 °C with PDIs below 0.26 when polymer concentrations of 1.0 mg mL^{-1} were used (Table 3). In the AB block copolymer group containing a fixed amount of the hydrophilic mPEGA (DP = 50) (Table 3, Entries 6–9 and 11), the hydrodynamic diameter of empty micelles spanned from 12 to 53 nm. As the length of the hydrophobic EHA block increased, the micelles exhibited a growth in diameter (**Figure 3**A). Other studies have also reported similar findings, indicating that there is a consistent correlation between the increase in hydrophobic chain length and the subsequent increase in hydrodynamic diameter.[24] This trend was similarly observed in AB block copolymers containing mPEGA (DP = 100) (Table 2, Entries 13 and 14). This trend can also be attributed to increasing molar masses of the polymers while simultaneously decreasing the hydrophilic proportions. To further understand the solution behavior and self-assembly, four polymers with either different molar mass or different hydrophilic/hydrophobic ratio were synthesized and analyzed (Figure 3B). P(mPEGA$_{25}$-*b*-EHA$_{53}$) with a mPEGA/EHA ratio of 1.2.1 and a molar mass of 11.6 kg mol^{-1} builds micelles with diameters of 36 nm, while P(mPEGA$_{50}$-*b*-EHA$_{116}$) with a similar hydrophobic content (mPEGA/EHA = 1:2.3) self-assembled to bigger micelles of 53 nm because of its increased molar mass of 18.9 kg mol^{-1}. With P(mPEGA$_{100}$-*b*-EHA$_{24}$) having a similar molar mass of 19.5 kg mol^{-1} but a higher hydrophilic content, the micelle sizes were decreased to 32 nm. The same decrease in micelle diameter was obtained between P(mPEGA$_{50}$-*b*-EHA$_{11}$) (12 nm) and P(mPEGA$_{25}$-*b*-EHA$_{53}$) (36 nm) having a similar molar mass but P(mPEGA$_{50}$-*b*-EHA$_{11}$) a much higher hydrophilicity verifying that except from molar mass the hydrophilic/hydrophobic ratio has a major effect on the self-assembly of the synthesized polymers. For our polymers we assume that polymers with a shorter hydrophilic block of mPEGA have also a smaller head group area at the amphiphilic interface. Following this, larger micelles are to be formed according to the packing parameter concept.

When comparing di- and triblock copolymers with similar hydrophilic to hydrophobic ratios of 1 and target DPs of mPEGA and EHA, i.e., P(mPEGA$_{50}$-*b*-EHA$_{50}$) and P(mPEGA$_{25}$-*b*-EHA$_{55}$-*b*-mPEGA$_{25}$), they exhibit similar hydrodynamic diameters (35 and 38 nm, respectively). However, P(EHA$_{50}$-*b*-mPEGA$_{50}$) block copolymer (Table 3, Entry 10), also with a mPEGA/EHA ratio of 1, displays a larger hydrodynamic diameter compared to the two aforementioned block copolymers, probably due to its less controlled synthesis leading to EHA homopolymer residues.

It is worth noting that also the distribution of both monomers along the polymer chain had an influence on the self-assembly of the polymer. The synthesis of P(mPEGA$_{20}$-*st*-EHA$_{48}$) through random polymerization resulted in the formation of considerably larger micelles (184 nm) compared to P(mPEGA$_{25}$-*b*-EHA$_{53}$) synthesized through block copolymerization (36 nm) (Table 3, Entries 4 and 5). This discrepancy can be attributed to the distinct core–shell structures of the block and random copolymers. Regarding the block copolymer P(mPEGA$_{25}$-*b*-EHA$_{53}$), the thick hydrophilic shell adequately stabilizes the core of the micelles in solution. On the other hand, the micelles formed by the random copolymer P(mPEGA$_{20}$-*st*-EHA$_{48}$) may not be sufficiently stabilized due to the relatively thin mPEGA shell surrounding the core, but still showing spherical micelles as verified by TEM measurements (**Figure 4**A). This indicates that the order of the hydrophobic and hydrophilic segments has a distinct impact on the size of the micelles, highlighting the positive impact of block arrangement on obtaining micelles with hydrodynamic diameter ranged between 10 and 100 nm. For polymers with hydrophilic/hydrophobic ratios of 1:0.2 to 1:0.5, micelles with sizes smaller than 32 nm were obtained, suitable for most effective drug delivery.[25] The stability behavior of the polymers for up to 30 d was investigated by DLS. According to the results, the hydrodynamic diameter of all polymers did not show substantial differences even after 30 d (Table S3, Supporting Information).

The hydrodynamic diameter of the polymers was measured at temperatures of 25, 60, 70, 80, 90 and 95 °C to investigate the thermoresponsive properties of polymers in solution (Figure S8 and Table S4, Supporting Information). The polymer's reaction to temperature fluctuations in an aqueous solution, leading to a sol-

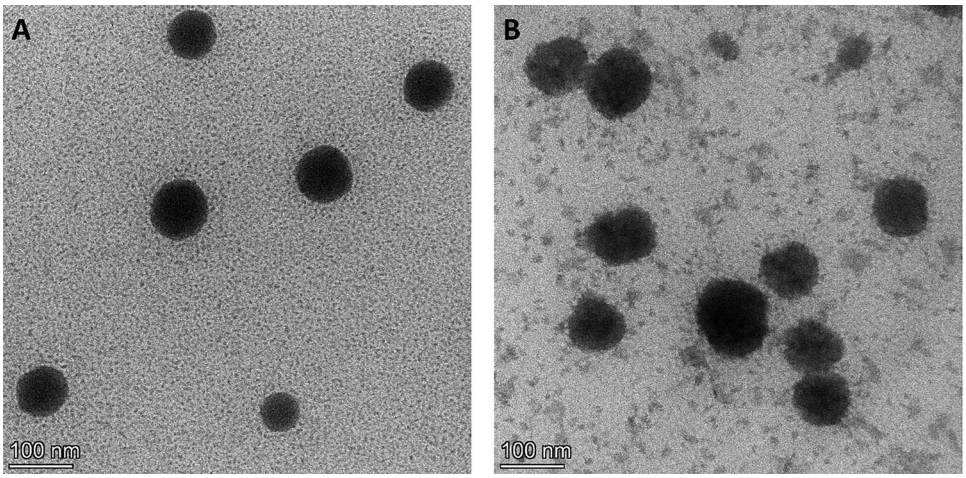

Figure 4. TEM measurements of spherical micelles from A) P(mPEGA$_{20}$-*st*-EHA$_{48}$) and B) P(mPEGA$_{25}$-*b*-EHA$_{55}$-*b*-mPEGA$_{25}$) (preparation see the Supporting Information).

ubility transition, can be identified through DLS. A substantial alteration in size due to aggregation of the polymer is anticipated at the cloud point temperature if polymers with lower critical solution temperatures (LCST) are present.[26] Such a significant alteration was observed for low-molecular weight polymers with low amounts of hydrophobic EHA (Table S4, Entries 3–5 and 7, Supporting Information). Previous studies have shown that mPEGA or oligoethylene glycol acrylate monomer with eight repeating units exhibit LCST values of 92 °C.[27] These findings are in accordance with the DLS studies conducted herein, when low amounts of EHA in low-molecular weight polymers did not affect the LCST effect of mPEGA: P(mPEGA$_{50}$-*b*-EHA$_{11}$) aggregated to big particles of around 3000 nm at 95 °C clearly showing the LCST behavior of the mPEGA block. Additionally, other polymers with low amounts of EHA and only up to 50 eq. of PEGA showed aggregate formation with sizes around 1500 nm and in which aggregates were smaller the more EHA was incorporated in the polymers indicating that the hydrophobic block has an influence on the LCST behavior of the hydrophilic block. Similar observations were made with higher molecular weight polymers. Increasing the molecular weight of the polymers or increasing the amount of EHA, both led to significant decrease in aggregate sizes of polymer solutions measured at 95 °C. Whereas P(mPEGA$_{111}$-*b*-EHA$_{24}$) (Table S4, Entry 9, Supporting Information) with a similar hydrophilic/hydrophobic ratio as P(mPEGA$_{50}$-*b*-EHA$_{16}$), but with a higher molecular weight, still showed quite big aggregates of around 500 nm at 95 °C, micelle sizes were only increased to 118–345 nm for all other high molecular weight AB or ABA polymers. P(mPEGA$_{111}$-*b*-EHA$_{110}$) with a high hydrophobicity and molecular weight and also P(mPEGA$_{50}$-*b*-EHA$_{116}$) only show a slight increase in micelle size at a temperature of 95 °C to 120 and 119 nm, respectively. It seems that for higher molecular weight polymers the LCST effect is only slightly pronounced.

In summary, all water-soluble AB, BA, and ABA block copolymers have shown a difference in size above 95 °C compared to their size at lower temperatures. Therefore, cloud points were above physiological temperature which are consequently not of major interest for drug delivery applications. However, to further study the impact of monomer composition and the molecular weight on the cloud point temperature, sizes were also measured at lower temperatures of 60–90 °C. Interestingly, an increase in temperature to up to 80 °C led to the formation of more uniform micelles for most of the polymers, which was reflected in a decrease in PDI (Table S4, Supporting Information).

Among the synthesized polymers, P(mPEGA$_{50}$-*b*-EHA$_{11}$) and P(mPEGA$_{50}$-*b*-EHA$_{16}$) have the highest hydrophilicity and show aggregation at a measuring temperature of 95 °C (Table S4, Entries 2 and 4, Supporting Information). P(mPEGA$_{50}$-*b*-EHA$_{26}$) with an increased EHA content showed aggregation already at a 90 °C measurement. We assume for low molecular weight AB polymers with 25 or 50 eq. mPEGA and up to 50 eq. EHA, an increase in hydrophobicity led to a slight decrease in the cloud point temperature. Similar or more pronounced effects were already observed in refs. [27b, 28].

P(mPEGA$_{100}$-*b*-EHA$_{24}$) with a similar hydrophilic/hydrophobic ratio as P(mPEGA$_{50}$-*b*-EHA$_{16}$), but a higher molecular weight shows a size increase already at 90 °C, indicating that higher molecular weights might also decrease the cloud point temperature. In contrast, P(mPEGA$_{100}$-*b*-EHA$_{111}$) with a higher hydrophobicity and molecular weight and also P(mPEGA$_{50}$-*b*-EHA$_{116}$) show size alteration solely at a temperature of 95 °C.

Comparing LCST behavior of P(EHA$_{50}$-*b*-mPEGA$_{50}$), P(mPEGA$_{25}$-*b*-EHA$_{55}$-*b*-mPEGA$_{25}$), and P(mPEGA$_{50}$-*b*-EHA$_{50}$) (Table S4, Entries 6, 7, and 11, Supporting Information) having almost similar hydrophilic/ hydrophobic ratios (1:1) and calculated molar masses (33.3 g mol^{-1}), only the latter one showed aggregation already at 90 °C. As discussed previously, EHA blocks being sandwiched between two mPEGA hydrophilic blocks which are located at the two ends of polymer can also contribute to enhancing the polymer's hydrophilicity. The same concept has also been reported in a work from Steinhauer et al. that by increasing the hydrophilicity of chain ends, an increase in LCST is observed.[29]

The random polymerization exhibited a notable variation in the uniform micelle structure upon heating, however, with the hydrodynamic diameter decreasing from 183.7 nm at 25 °C to 155.8 nm at 70 °C and more uniform micelles were formed as shown by a decrease in PDI from 0.2 (25 °C) to 0.03 (95 °C)

(Table S4, Entry 1, Supporting Information). No LCST behavior in this temperature range was observed for the random copolymer as sizes were only slightly increased to 223 °C at 95 °C.

The CMC value, an essential parameter for assessing micelle formation ability, was determined using Nile red as a fluorescent probe in spectroscopic analysis. CMC values are obtained by mixing increasing polymer concentrations with Nile red in water. Upon micelle formation and above the CMC, Nile red is dissolved in the micelles and causes a fluorescence signal (Figure S9, Supporting Information). The decrease in CMC value can be regarded as a reflection of the improved stability of micelles. Typically, polymeric micelles exhibit considerably lower CMC values (ranging from 10^{-6} to 10^{-7} M) compared to conventional small molecule micelles (ranging from 10^{-3} to 10^{-4} M).[30] Micelle solutions at low concentrations disintegrate without sufficient surfactant content. Thus a lower CMC is necessary to maintain the micelle structure and not force micellar destruction upon dilution by injecting the micelle into the bloodstream.[25] In this regard, the polymers synthesized in this study demonstrate suitable CMC values (ranging from 8 to 100 $\times 10^{-7}$ M) which aligns with the previous research findings on CMC values of polymeric micelles (Table 3).[16,25–27] CMC values of all P(mPEGA-*b*-EHA) copolymers fall within the range of 0.029–0.272 mg mL^{-1}. As shown in Figure 3, AB block copolymers with a fixed amount of the hydrophilic mPEGA block (DP = 50) (Table 3, Entries 6–9 and 11) show decreased CMC values with increasing hydrophobicity and thus higher amounts of EHA signifying an improvement in their structural stability. This finding is consistent with previous publications.[31] This suggests that the relative proportions of hydrophobic and hydrophilic monomers play a crucial role in determining the CMC and subsequent micelle formation.[32] Further evidence for an opposing trend in comparison to the hydrodynamic diameter of micelles is given by an increase in CMC when comparing P($mPEGA_{50}$-*b*-EHA_{11}) (CMC = 0.272 mg mL^{-1}) and P($mPEGA_{25}$-*b*-EHA_{53}) (CMC = 0.041 mg mL^{-1}) or P($mPEGA_{100}$-*b*-EHA_{24}) (CMC = 0.118 mg mL^{-1}) and P($mPEGA_{50}$-*b*-EHA_{116}) (CMC = 0.057 mg mL^{-1}) with similar molar masses but P($mPEGA_{50}$-*b*-EHA_{11}) and P($mPEGA_{100}$-*b*-EHA_{24}) having a higher hydrophilicity, respectively (Figure 3B).

Conversely, when it comes to AB block copolymers with higher molecular weight containing a constant amount of the hydrophilic mPEGA block (DP = 100) (Table 3, Entries 12 and 13), they do not exhibit a similar pattern. In this case, the CMC values (0.118 and 0.138 mg mL^{-1}, respectively) decrease as the hydrophobic components increases. Additionally, these polymers exhibit higher CMC values than some other polymers with lower molecular weight, probably due to their higher molecular weight, however, the influence of the hydrophobic content seems to be more crucial since polymers bearing mPEGA (DP = 50) and only low amounts of EHA have much higher CMCs (Table 2, Entries 6 and 7). The investigation of the ABA copolymer, P($mPEGA_{25}$-*b*-EHA_{55}-*b*-$mPEGA_{25}$) (Table 2, Entry 14), with a fixed hydrophilic/hydrophobic ratio of 1:1 revealed an even lower CMC value (0.029 mg mL^{-1}) than similar AB polymers (Figure 3A). The separation of the hydrophilic segment into two blocks and positioning the hydrophobic block in the middle led to improved self-assembly of the polymer into spherical micelles as also observed during TEM measurements (Figure 4B). In contrast, the BAB block copolymer P(EHA_{25}-*b*-$mPEGA_{50}$-*b*-EHA_{25}) (Table 3, Entry 15) with the hydrophilic segment in the middle was observed to be insoluble in water. The favorable solubility achieved by the ABA copolymer, with the hydrophobic segment in the middle, corroborates similar findings reported in other research studies.[25] Comparing the results of two copolymers, namely P($mPEGA_{20}$-*st*-EHA_{48}) synthesized through random polymerization and P($mPEGA_{25}$-*b*-EHA_{53}) synthesized via block copolymerization, with a similar mPEGA/EHA ratio, it is observed that they exhibit closely comparable CMC values (0.036 and 0.041 mg mL^{-1}). These results indicate that the dominating factors influencing CMCs are the monomer ratios and to some extent the molar masses.

2.3. Cell Viability Evaluation of Copolymers

The in vitro cell viability assessment of copolymers was performed using the MTS and CV assays using the ARPE-19 cell line which is a spontaneously arising retinal pigment epithelial (RPE) cell line. The developed MTS reagent can be readily reduced by viable cells, leading to the production of formazan products that are soluble in the cell culture medium to determine the quantity of viable cells in multiwell plates.[33] MTS results showed excellent cytocompatibility of polymers at all concentrations (including 1000 μg mL^{-1}) after 24 h (**Figure 5**) and 48 h (Figure S10, Supporting Information) of incubation. After 24 h incubation with P(EHA_{50}-*b*-$mPEGA_{50}$) and P($mPEGA_{25}$-*b*-EHA_{55}-*b*-$mPEGA_{25}$) at the two highest concentrations (100 and 1000 μg mL^{-1}), the cell viability was lower compared to other concentrations. However, it is important to note that even though the viability is slightly reduced, it remains within the acceptable range, indicating that the cells still maintain at a satisfactory level of viability. When cells undergo cell death, the adherent cells detach from cell culture plates. To identify the cells that maintain adherence, a common approach involves staining the attached cells with crystal violet dye, which has an affinity for proteins and DNA. As a result, cells that have experienced cell death lose their adherence and are consequently lost from the cell population, leading to a decrease in the amount of crystal violet staining observed in the culture.[34] The results obtained from the CV assay indicated that there was no substantial difference in cell density between the groups treated with polymers and the control cells, at both the 24 h time point (Figure 4) and the 48 h time point (Figure S10, Supporting Information). This observation held true even when considering the highest two concentrations tested further showing the neglectable slightly worse results from MTS assay.

To evaluate cell viability with an additional method, all groups were treated with Calcein-AM (green)/ PI (red) staining to stain live and dead cells, respectively. Evidence of the absence of apoptosis in the cells was found, as demonstrated by the lack of detectable red fluorescence in the images obtained from the AF555 channel (**Figure 6** and Figure S11, Supporting Information). Furthermore, only green fluorescence is observed in the images captured using the eGFP channel, proofing viable cells. In addition, the morphology of cells appears to be comparable to that of the control group, indicating excellent biocompatibility.

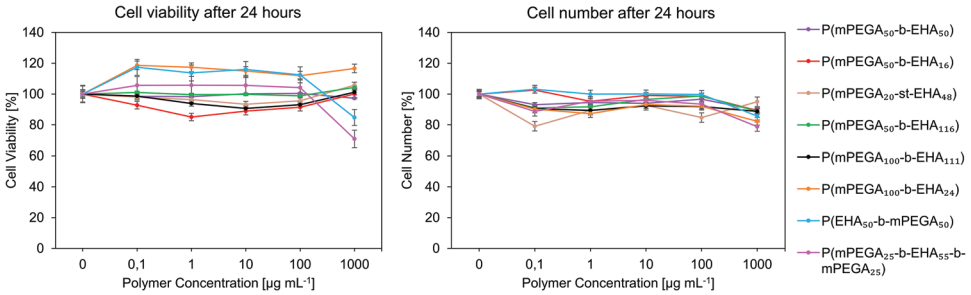

Figure 5. MTS and CV assays were performed with different copolymers and concentrations using ARPE-19 cell line. The respective culture duration is 24 h ($n = 3 \pm$ SD).

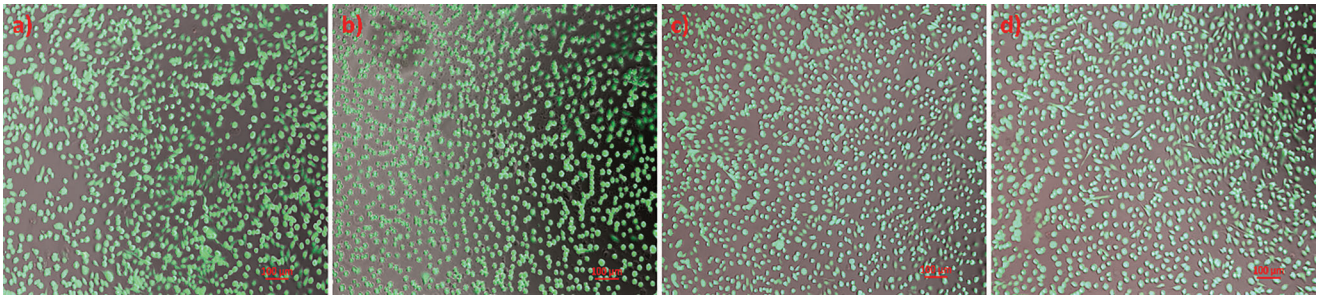

Figure 6. ARPE-19 cell line subjected to Calcein-AM (green) and PI (red) staining after incubation with polymers. a) Control, b) P(mPEGA$_{50}$-*b*-EHA$_{116}$), c) P(mPEGA$_{100}$-*b*-EHA$_{111}$), and d) P(mPEGA$_{100}$-*b*-EHA$_{24}$) at their highest concentration (1000 µg mL^{-1}) after 48 h. The resulting images are merged from bright field, AF555 (PI), and eGFP (Calcein-AM) channels and a scale bar of 100 µm was included for reference.

3. Conclusion

In this study, the solution behavior of copolymers consisting of hydrophilic, comb-shape mPEGA, and hydrophobic, branched EHA with predetermined and controlled chemical structural parameters was investigated. Polymers were synthesized by Cu(0)-mediated SET-LRP resulting in AB, BA, ABA, and BAB block copolymers as well as a random copolymer. The obtained copolymers showed molar masses between 7.7 and 25.5 kg mol^{-1} and successful block copolymer formation was proven. Due to a better control and preciseness of mPEGA polymerizations, AB polymers with mPEGA as the first block showed better results in terms of polydispersity (≤1.25) than the ones in which chain extension of P(EHA) was performed. To study the solution behavior, various characterization techniques were employed, revealing uniform particle sizes in dependence of the molar mass and mPEGA/EHA ratio. In addition, the impact of hydrophilic/hydrophobic ratio and molar masses on CMC values as an indicator for micelle stability were studied. All studied block copolymers self-assembled to favorable micelle sizes between 12 and 55 nm, revealing that the branched hydrophobic structure of EHA facilitates self-assembly to stable and uniform micelles. Polymers having a high hydrophilic content showed reduced hydrodynamic diameter of micelles and an increase in their CMC, while polymers with more hydrophobic content showed the opposite trends. When also considering molar masses, polymers with higher molecular weights also showed increased hydrodynamic diameter and in general higher CMC values. Interestingly, a synthesized ABA polymer showed a similar hydrodynamic diameter and a slightly lower CMC as the AB copolymers with an identical hydrophobic to hydrophilic ratio of 1. This can be explained by separating the hydrophilic segment that has a negative influence on the CMC value into two parts reducing its impact on polymer self-assembly, consequently, acting more like a polymer with a higher hydrophobic content. Both AB and ABA polymers with a hydrophobic to hydrophilic ratio of 1 showed a perfect balance of micelle sizes and CMC values. In case passing through less permeable tumor tissue is desired, hydrodynamic diameters can easily be decreased by incorporating more mPEGA monomers in the block copolymers. Furthermore, in vitro experiments demonstrated a desirable biocompatibility of P(mPEGA-*b*-EHA) diblock and triblock copolymers. For designing a successful nanocarrier, materials must exhibit low toxicity combined with size uniformity and colloidal stability. In this paper, materials with such features were synthesized and characterized for using these novel amphiphilic polymers as nanocarrier in drug delivery technologies.

Supporting Information

Supporting Information is available from the Wiley Online Library or from the author.

Acknowledgements

Y.P.H. and S.Ç. contributed equally to this work. The authors gratefully acknowledge the core facility SRF AMICA (Stuttgart Research Focus Advanced Materials Innovation and Characterization) at the University of Stuttgart for their support and assistance in this work. The authors thank

Lea-Sophie Hornberger and Philipp Weingarten for their help with NMR and SEC measurements. Y.P.H. and F.A. are thankful for funding by the Federal Ministry of Education and Research (BMBF) and the Baden-Württemberg Ministry of Science as part of the Excellence Strategy of the German Federal and State Governments. This work was supported by a postdoc fellowship of the German Academic Exchange Service (DAAD).

Open access funding enabled and organized by Projekt DEAL.

Conflict of Interest

The authors declare no conflict of interest.

Data Availability Statement

The data that support the findings of this study are available from the corresponding author upon reasonable request.

Keywords

amphiphilic polymers, block copolymers, living radical polymerization, micelles, poly(ethylenglycol), SET-LRP

Received: June 30, 2023
Revised: August 17, 2023
Published online: September 19, 2023

[1] A. Rösler, G. W. M. Vandermeulen, H.-A. Klok, *Adv. Drug Deliv. Rev.* **2012**, *64*, 270.
[2] G. S. Kwon, T. Okano, *Adv. Drug Delivery Rev.* **1996**, *21*, 107.
[3] X. F. Liang, H. J. Wang, H. Luo, H. Tian, B. B. Zhang, L. i. J. Hao, J. I. Teng, J. Chang, *Langmuir* **2008**, *24*, 7147.
[4] J. S. Lee, J. Feijen, *J. Controlled Release* **2012**, *161*, 473.
[5] K. Madaan, S. Kumar, N. Poonia, V. Lather, D. Pandita, *J. Pharm. Bioallied Sci.* **2014**, *6*, 139.
[6] C. Demetzos, C. Demetzos, *Pharmaceutical nanotechnology: fundamentals and practical applications*, **2016**, pp. 77–145.
[7] K. Letchford, H. Burt, *Eur. J. Pharm. Biopharm.* **2007**, *65*, 259.
[8] F. Perin, A. Motta, D. Maniglio, *Mater. Sci. Eng., C* **2021**, *123*, 111952.
[9] a) D. R. Perinelli, M. Cespi, N. Lorusso, G. F. Palmieri, G. Bonacucina, P. Blasi, *Langmuir* **2020**, *36*, 5745; b) R. Nagarajan, *Self-Assembly: From Surfactants to Nanoparticles*, John Wiley and Sons, New York **2019**; c) R. Nagarajan, *Langmuir* **2002**, *18*, 31.
[10] a) Á. G. García, A. Ianiro, R. Tuinier, *ACS Omega* **2018**, *3*, 17976; b) R. Lund, L. Willner, D. Richter, E. E. Dormidontova, *Macromolecules* **2006**, *39*, 4566.
[11] M. Ghezzi, S. Pescina, C. Padula, P. Santi, E. Del Favero, L. Cantù, S. Nicoli, *J. Controlled Release* **2021**, *332*, 312.
[12] a) A. Mandal, R. Bisht, I. D. Rupenthal, A. K. Mitra, *J. Controlled Release* **2017**, *248*, 96; b) H. Cabral, Y. Matsumoto, K. Mizuno, Q. Chen, M. Murakami, M. Kimura, Y. Terada, M. R. Kano, K. Miyazono, M. Uesaka, N. Nishiyama, K. Kataoka, *Nat. Nanotechnol.* **2011**, *6*, 815.
[13] M. L. Adams, A. Lavasanifar, G. S. Kwon, *J. Pharm. Sci.* **2003**, *92*, 1343.
[14] X.-B. Xiong, Z. Binkhathlan, O. Molavi, A. Lavasanifar, *Acta Biomater.* **2012**, *8*, 2017.
[15] S. R. Samanta, M. E. Levere, V. Percec, *Polym. Chem.* **2013**, *4*, 3212.
[16] A. Anastasaki, V. Nikolaou, D. M. Haddleton, *Polym. Chem.* **2016**, *7*, 1002.
[17] A. Anastasaki, V. Nikolaou, G. Nurumbetov, P. Wilson, K. Kempe, J. F. Quinn, T. P. Davis, M. R. Whittaker, D. M. Haddleton, *Chem. Rev.* **2016**, *116*, 835.
[18] B. Müller, W. Rath, *Formulierung von Kleb- und Dichtstoffen: das kompetente Lehrbuch für Studium und Praxis*, Vincentz, **2004**.
[19] a) Y. Zhou, F. Liu, L. Liu, X. Qiu, M. Ye, H. Pan, H. Liu, *Food Chem.* **2022**, *397*, 133830; b) L. Scermino, A. Fabozzi, G. De Tommaso, A. J. M. Valente, M. Iuliano, L. Paduano, G. D'errico, *J. Mol. Liq.* **2020**, *316*, 113799; c) Y. Li, H. Zhang, M. Bao, Q. Chen, *J. Dispersion Sci.* **2012**, *33*, 1437.
[20] D. Ibrahim, C. Luigi, *Process for the Production of Acrylic Acid Esters*, U.S. *Patent No. 2*,881,205, **1959**.
[21] G. Lligadas, S. Grama, V. Percec, *Biomacromolecules* **2017**, *18*, 2981.
[22] L. Voorhaar, S. Wallyn, F. E. Du Prez, R. Hoogenboom, *Polym. Chem.* **2014**, *5*, 4268.
[23] a) R. Evans, G. Dal Poggetto, M. Nilsson, G. A. Morris, *Anal. Chem.* **2018**, *90*, 3987; b) R. Evans, Z. Deng, A. K. Rogerson, A. S. McLachlan, J. J. Richards, M. Nilsson, G. A. Morris, *Angew. Chem., Int. Ed.* **2013**, *52*, 3199.
[24] Y. Wang, M. J. Van Steenbergen, N. Beztsinna, Y. Shi, T. Lammers, C. F. Van Nostrum, W. E. Hennink, *J. Controlled Release* **2020**, *328*, 970.
[25] R. Hoogenboom, F. Wiesbrock, H. Huang, M. A. M. Leenen, H. M. L. Thijs, S. F. G. M. Van Nispen, M. Van Der Loop, C.-A. Fustin, A. M. Jonas, J.-F. Gohy, U. S. Schubert, *Macromolecules* **2006**, *39*, 4719.
[26] a) K. Bebis, M. W. Jones, D. M. Haddleton, M. I. Gibson, *Polym. Chem.* **2011**, *2*, 975; b) G. M. L. Consoli, M. L. Giuffrida, C. Satriano, T. Musumeci, G. Forte, S. Petralia, *Chem. Commun.* **2022**, *58*, 3126.
[27] a) C. Boyer, M. R. Whittaker, M. Luzon, T. P. Davis, *Macromolecules* **2009**, *42*, 6917; b) G. Vancoillie, D. Frank, R. Hoogenboom, *Prog. Polym. Sci.* **2014**, *39*, 1074.
[28] a) C. Weber, R. Hoogenboom, U. S. Schubert, *Prog. Polym. Sci.* **2012**, *37*, 686; b) N. Zhang, S. Salzinger, B. Rieger, *Macromolecules* **2012**, *45*, 9751; c) F. Adams, P. T. Altenbuchner, P. D. L. Werz, B. Rieger, *RSC Adv.* **2016**, *6*, 78750.
[29] W. Steinhauer, R. Hoogenboom, H. Keul, M. Moeller, *Macromolecules* **2010**, *43*, 7041.
[30] Y. Lu, E. Zhang, J. Yang, Z. Cao, *Nano Res.* **2018**, *11*, 4985.
[31] a) N. Kang, J.-C. Leroux, *Polymer* **2004**, *45*, 8967; b) Y. Hussein, M. Youssry, *Materials* **2018**, *11*, 688; c) M. Bagheri, J. Bresseleers, A. Varela-Moreira, O. Sandre, S. A. Meeuwissen, R. M. Schiffelers, J. M. Metselaar, C. F. Van Nostrum, J. C. M. Van Hest, W. E. Hennink, *Langmuir* **2018**, *34*, 15495; d) C. Kim, S. C. Lee, J. H. Shin, J.-S. Yoon, I. C. Kwon, S. Y. Jeong, *Macromolecules* **2000**, *33*, 7448.
[32] Y. u. Shao, Y.-G. Jia, C. Shi, J. Luo, X. X. Zhu, *Biomacromolecules* **2014**, *15*, 1837.
[33] a) C. J. Goodwin, S. J. Holt, S. Downes, N. J. Marshall, *J. Immunol. Methods* **1995**, *179*, 95; b) T. L. Riss, R. A. Moravec, A. L. Niles, S. Duellman, H. A. Benink, T. J. Worzella, L. Minor, *Assay Guidance Manual [Internet]* **2016**.
[34] M. Feoktistova, P. Geserick, M. Leverkus, *Cold Spring Harb Protoc* **2016**, *2016*, 343.

